Comparison of Flux-Switching Machines With and Without Permanent Magnets

Christopher H. T. Lee, K. T. Chau, and C. C. Chan*
(Department of Electrical and Electronic Engineering, The University of Hong Kong, Hong Kong, China)

Abstract: In this paper, three advanced flux-switching (FS) machines, namely the radial-field flux-switching permanent-magnet (RF-FSPM) machine, the radial-field flux-switching DC-field (RF-FSDC) machine, and the axial-field FSDC (AF-FSDC) machine are quantitatively compared. Upon the installation of the high-energy-density PM materials, the RF-FSPM machine can definitely provide the superior torque performances as compared to its magnetless counterparts. However, the PM machines suffer from two major fundamental problems, namely the high material costs, and the uncontrollable flux density. By utilizing the concept of axial-field structure, the AF-FSDC machine can offer comparable torque performance as the RF-FSPM machine. Hence, with the consideration of the cost-effectiveness and the control flexibility, the magnetless AF-FSDC machine has exhibited promising potential in various applications.

Keywords: Flux-switching, magnetless, radial-field, axial-field, cost-effectiveness.

1 Introduction

Because of the enhancing concerns on the energy utilization as well as the environmental protection, the development of the electric machines has been drastically accelerating[1-3]. To be specific, the electric machines generally need to provide various distinctive characteristics, including high efficiency, high power density, high controllability, wide-speed range, and maintenance-free operation[4-6]. The flux-switching permanent-magnet (FSPM) machines, which can accomplish most of the goals, have drawn many attentions in the past few years[7-9]. However, due to the fluctuating supply of the PM materials, the construction costs of the PM machines have soared tremendously[10-12]. Hence, the magnetless machines, which enjoy the absolute advantage of lower material cost, have become more popular recently[13-15].

Without installation of any high-energy-density PM materials, the magnetless machines undoubtedly suffer from relatively lower torque density. To improve the situation, the axial-field (AF) structure, which utilizes the radial length as active part for torque generation, has been proposed[16-18]. Based on the AF structure, larger torque production area is resulted so that the AF machines can greatly improve its torque density as compared with its radial-field (RF) counterparts[19-21]. Even though the magnetless AF machines have been proposed, the quantitative comparisons among the PM and magnetless candidates based on the two structures are still literally absent.

The purpose of this paper is to quantitatively compare the representative FS machines, namely the RF-FSPM machine, the magnetless RF flux-switching DC-field (FSDC) machine, and the magnetless AF-FSDC machine. The design criteria and operating principles of all these FS machines will be discussed. All the machines are designed based on the fair conditions, while their key machine performances will be analyzed by using the finite element method (FEM).

2 Flux-switching machines

Fig.1 shows the topologies of the three FS machines, namely the 12/10-pole RF-FSPM machine, the 12/10-pole RF-FSDC machine, and the 12/10-pole AF-FSDC machine. Both the RF-FSPM machine and the RF-FSDC machine employ the outer-stator inner-rotor structure, while the AF-FSDC machine employs the sandwiched-stator double-sided-rotor structure. The stator and rotor construction of the proposed machines are similar to those of the commonly employed machines[3].

Because all these FS machines have the same principle of operation, the design equations such as the pole arrangement can be extended from that of the well-established RF-FSPM machine[8]. Hence, the pole arrangements for all the FS machines are governed by

$$\begin{cases} N_s = 2mk \\ N_r = N_s \pm k \end{cases} \tag{1}$$

* Corresponding author, E-mail:ktchau@eee.hku.hk.
Supported by a grant (Project No. 17200614) from the Hong Kong Research Grants Council, Hong Kong Special Administrative Region, China.

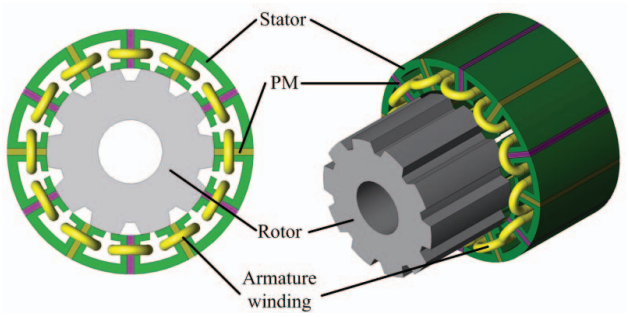

(a) RF-FSPM

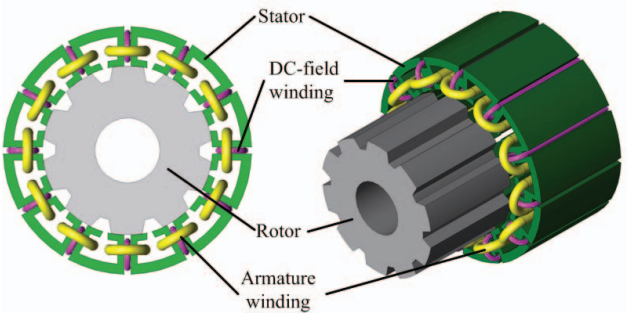

(b) RF-FSDC

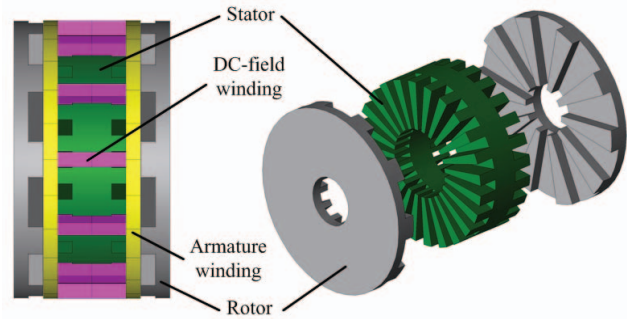

(c) AF-FSDC

Fig.1 Proposed FS machines

where N_s is the number of stator poles, N_r is the number of rotor poles, m is the number of armature phases and k is any integer. By selecting m=3, and k = 2, this ends up with N_s = 12, N_r = 10 and comes up with the structure for all three machines.

The FSPM machine employs only one type of winding, namely the armature winding, while the FSDC machines employ instead two types of windings, namely the armature winding and the DC-field winding. All the armature windings adopt the concentrated winding arrangement, while the DC-field windings adopt the toroidal winding arrangement. Based on the toroidal winding arrangement, the DC-field of the FSDC machines can emulate the flux patterns offered by the PM excitation does, so that all the machines can achieve the bipolar flux-linkage characteristics.

The flux flow patterns of the RF-FSPM machine, the RF-FSDC machine, and the AF-FSDC machine are shown in Fig.2, Fig.3, and Fig.4, respectively. To be specific, when the rotor of the FS machine rotates from position 1 to 2, the flux-linkages interchange its polarities accordingly. Therefore, the bipolar flux-linkage characteristics are achieved so that higher power and torque densities can be resulted.

Unlike the RF machines that employ the single-stator single-rotor structure, the AF-FSDC machine instead adopts the single-stator double-rotor structure. It should be noted that the AF machine is purposely designed to have the symmetrical topology so that equal torque can be produced by the two sided-segments. Therefore, the two separated rotors can be connected to the load together, such that higher torque density can be achieved. Consequently, to simplify the control algorithm, the two armature winding sets can be purposely connected in series.

To offer the fair environment for comparisons, all the major machine dimensions, namely the radial outside diameters, the radial inside diameters, the axial stack lengths, and the airgap lengths are set equal. In the meantime, to avoid the magnetic saturations as well as the core losses, the pole arcs, the pole heights, the slot-fill factors, and the current densities are optimized accordingly.

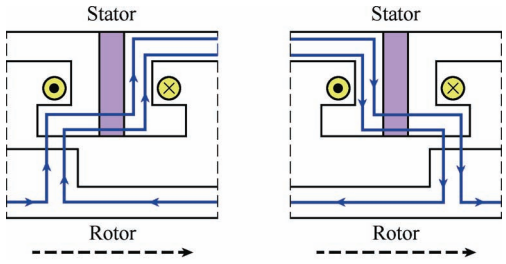

(a) Position 1 (b) Position 2

Fig.2 Flux flow pattern of RF-FSPM machine

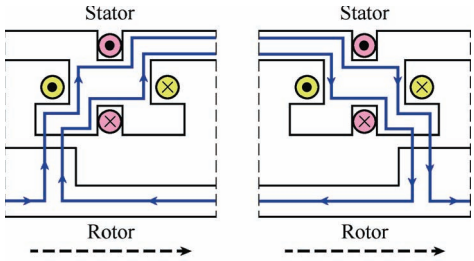

(a) Position 1 (b) Position 2

Fig.3 Flux flow pattern of RF-FSDC machine

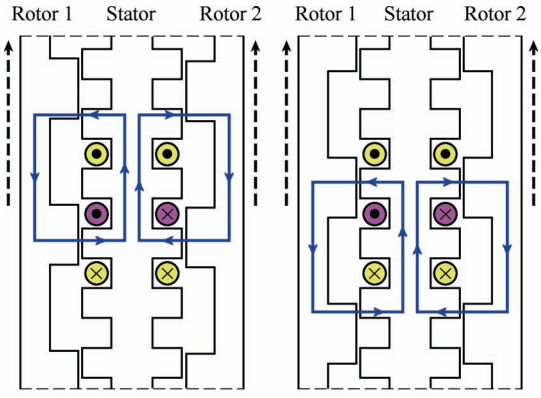

(a) Position 1 (b) Position 2

Fig.4 Flux flow pattern of AF-FSDC machine

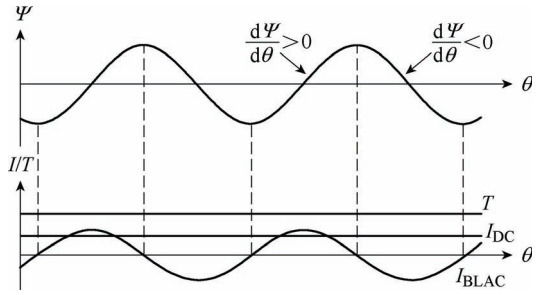

Fig.5 Theoretical bipolar conduction scheme

3 Operating principles

All these FS machines can be operated with the bipolar conduction operation, which is commonly employed for the conventional FSPM machine[7]. To be specific, the sinusoidal armature current I_{BLAC} is applied in accordance with the status of the bipolar flux-linkage Ψ, so that the positive electromagnetic torque T is produced. This operation is so-called as the brushless AC (BLAC) conduction scheme, as shown in Fig.5. With the BLAC conduction scheme, the sinusoidal-like machine can perfectly match the injected armature currents with its back electromotive force (EMF) waveforms, so that the torque ripple can be purposely minimized. The corresponding sinusoidal armature currents can be described as

$$\begin{cases} i_a = I_{\max} \sin\theta \\ i_b = I_{\max} \sin(\theta + (2\pi/3)) \\ i_c = I_{\max} \sin(\theta - (2\pi/3)) \end{cases} \quad (2)$$

where i_a, i_b, i_c and $I_{\max}$ are the corresponding armature currents and the maximum value of the phase currents, respectively.

On the installation of the strong PM materials, the RF-FSPM machine can provide very minimal flux controllability and hence this type of machine is not capable for wide-speed range operation. On the other hand, the FSDC machines install with the independent DC-field winding I_{DC} for flux regulation and it can be expected that these advanced magnetless candidates can provide outstanding flux-weakening performances to fulfill various needs. In addition to the flux-weakening capability, the DC-field can be utilized to achieve the flux-strengthening purposes. It can be anticipated that the FSDC machines can regulate its DC-field excitation to boost up its torque density in a short period of time, in order to accomplish some specific tasks, e.g., acceleration or hill-climbing for electric vehicles[4].

4 Machine performance analysis

All the three FS machines are analyzed and compared based on the fair conditions while the key design data of these machines are listed in Table 1. By utilizing the FEM, all machine performances can be simulated and then quantitatively compared. In this paper, JMAG-Designer is adopted to perform the FEM analysis.

First of all, the flux-linkages of all machines are shown in Fig.6. It can be seen that all the flux-linkages are well balanced with bipolar characteristics among three-phase patterns. Each of the flux-linkages exhibits the symmetrical pattern without significant distortion. The results confirm that the pole-pair arrangements and the winding configurations of all three FS machines are correctly designed.

Table 1 Key machine design data

	RF-FSPM	RF-FSDC	AF-FSDC
Radial outside diameter/mm	381.0	381.0	381.0
Radial inside diameter/mm	100.0	100.0	100.0
Airgap length/mm	0.5	0.5	0.5
Axial stack length/mm	195.0	195.0	195.0
Rotor pole number	12	12	12
Stator pole number	10	10	10
No. of phases	3	3	3
Excitation	PM	DC-field	DC-field
Slot-fill factor(%)	60	60	60
No. of armature turns	100	100	140

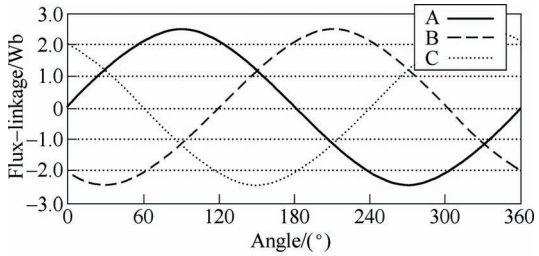

(a) RF-FSPM

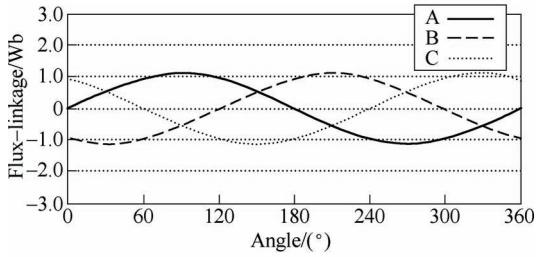

(b) RF-FSDC

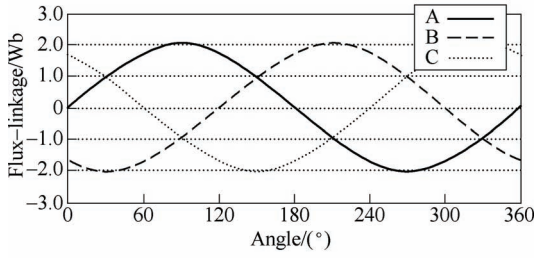

(c) AF-FSDC

Fig.6 Flux linkages waveforms

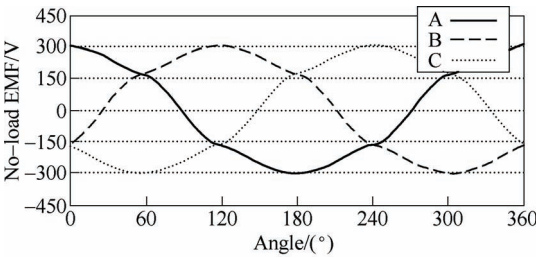

(a) RF-FSPM

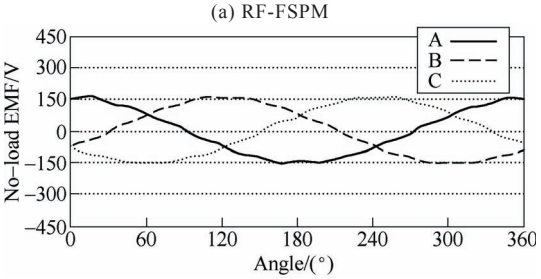

(b) RF-FSDC

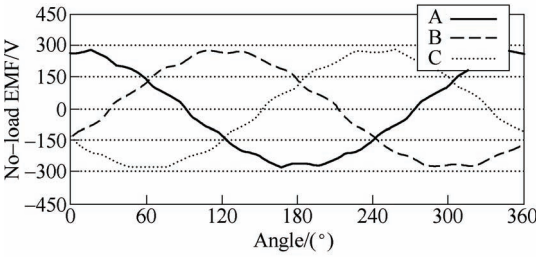

(c) AF-FSDC

Fig.7 No-load EMF waveforms

Secondly, the no-load EMF waveforms of these FS machines at the base speed of 300r/min with either PM excitation or the rated DC-field excitation of 5 A/mm^2 are shown in Fig.7. The results show that all FS machines obtain the sinusoidal-like patterns, which are suitable for the BLAC conduction scheme to produce the smoother torque performance. In the meantime, as expected, without the high-energy-density PM materials, the no-load EMFs generated by the FSDC machines are relatively lower than those by the FSPM machine are. Yet, by employing the AF structure, the AF-FSDC machine can achieve better no-load EMF performance than the RF counterpart can. Hence, it is expected that the power level of the AF-FSDC machine is comparable to that offered by the RF-FSPM machine.

Next, to compare the flux-weakening performance of the FS machines, the no-load EMF waveforms of RF-FSPM machine, RF-FSDC machine, and AF-FSDC machine at various speeds are also carried out as shown in Fig.8, Fig.9, and Fig.10, respectively. Not surprisingly, the magnitudes of the no-load EMFs of all three machines increase in accordance to the operating speeds. As aforementioned, the PM materials suffer from poor flux regulation performance so that the FSPM machine has very weak flux-weakening characteristics, as compared with the advanced magnetless counterparts. On the other hand, with the support of the controllable DC-field excitation, the FSDC machines can both regulate their no-load EMFs effectively, so that the magnitudes can be maintained constant throughout a wide-speed range.

In the third place, the steady output torques of the proposed FS machines are calculated as shown in Fig.11. It can be seen that the rated average torques at rated conditions of the RF-FSPM machine, the RF-FSDC machine, and the AF-FSDC machine are 202.3N·m, 98.1N·m, and 152.4N·m, respectively. As expected, upon the installation of the high-energy-density PM materials, the RF-FSPM machine can

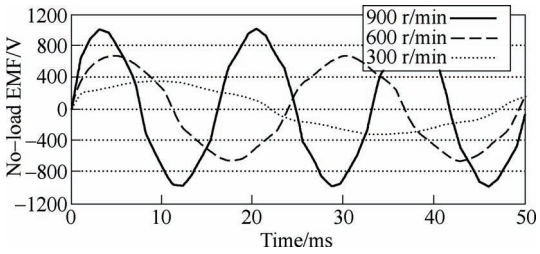

Fig.8 No-load EMFs at various speeds of RF-FSPM

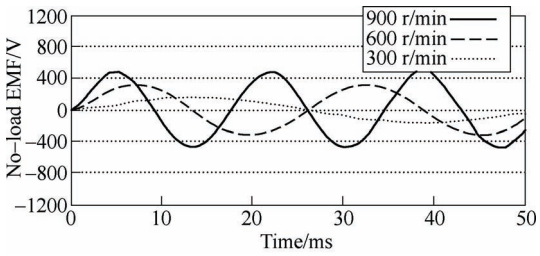

(a) Without flux regulation

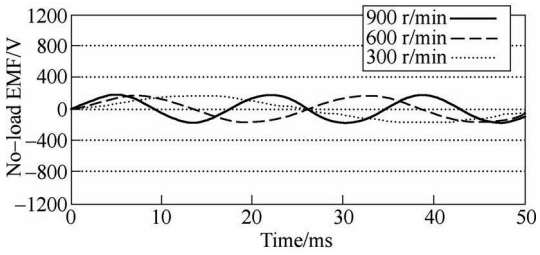

(b) With flux regulation

Fig.9 No-load EMFs at various speeds of RF-FSDC

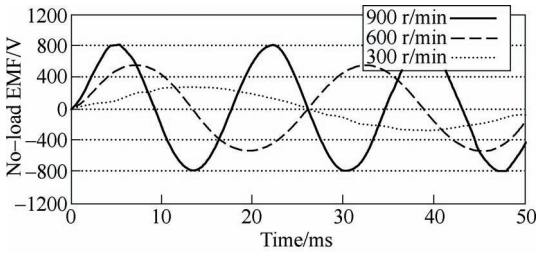

(a) Without flux regulation

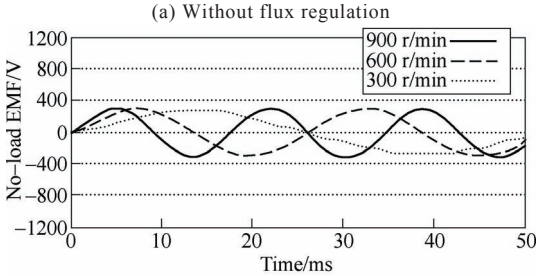

(b) With flux regulation

Fig.10 No-load EMFs at various speeds of AF-FSDC

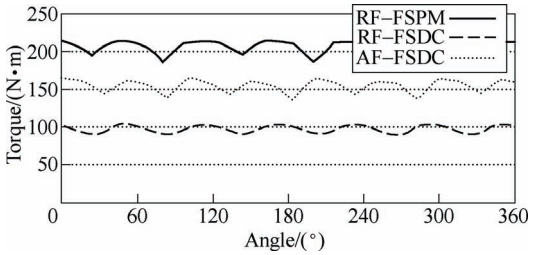

Fig.11 Rated steady torque waveforms

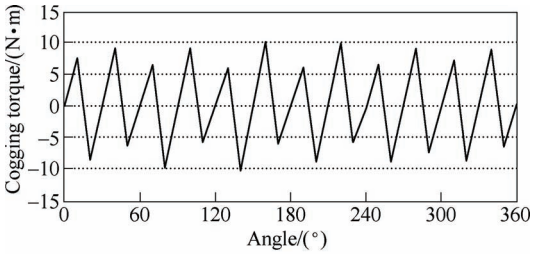

(a) RF-FSPM

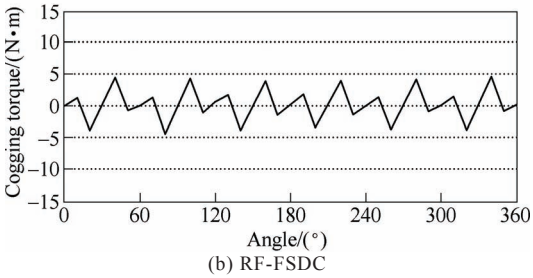

(b) RF-FSDC

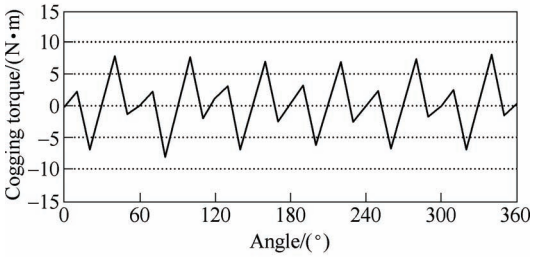

(c) AF-FSDC

Fig.12 Cogging torques at rated conditions

achieve the highest torque value among them. In the meantime, by fully utilizing the radial area for torque production, the AF-FSDC machine can achieve far better torque performance than the RF magnetless counterpart can. In particular, as compared with the RF-FSDC machine, the torque enhancement through the AF structure is about 55.4%, and this value is considered comparable to the PM one.

Next, in addition to the average torque value, the torque ripples of the machines are also well studied. The obtained torque ripples of the RF-FSPM machine, the RF-FSDC machine, and the AF-FSDC machine are 12.8%, 17.6% and 15.1%, respectively, which are similar to the commonly employed stator-PM machines[6]. In the meantime, the cogging torques of the RF-FSPM machine, the RF-FSDC machine, and the AF-FSDC machine are shown in Fig.12, where their peak amplitudes are found to be 10.1N·m, 4.8N·m, and 7.7N·m, respectively. These values are within the acceptable range, which are only 5.0%, 4.9% and 5.1% of their corresponding rated torques.

Then, the torque boosting characteristics of the FS machines are also carefully studied. As suggested, the FSDC machines can utilize their DC-field excitation for flux-strengthening, while their boosted torque performances with the DC-field excitation of 10 A/mm^2 are shown in Fig.13. It can be seen that the boosted average torques of the RF-FSDC machine and the AF-FSDC machine are 114.2N·m, and 181.6N·m, respectively, with torque ripples of 23.2% and 21.2 % respectively. In the meantime, the cogging torques of the RF-FSDC machine and the AF-FSDC machine at boosted conditions are shown in Fig.14, where their peak amplitudes are found to be 8.1N·m, and 14.1N·m, respectively. These values are within the acceptable range, which are only 7.1% and 7.7% of their corresponding boosted torques. As compared with the rated torque conditions, as shown in Fig. 11, the RF-FSDC machine and the AF-FSDC machine can improve their torque values by 16.4% and 19.2%, respectively. In particular, to avoid overheating the electric machines, the torque boosting mode should be employed for short period of time, say around 10-15 mins.

Finally, the concept of the cost-effectiveness is also employed to improve the comprehensiveness of the comparison. The material costs of the FS machine are calculated based on the raw materials of the current market prices, while the key comparison of

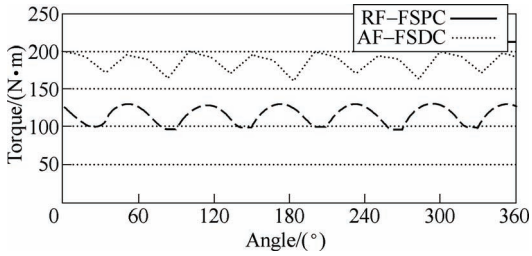

Fig.13 Boosted steady torque waveforms

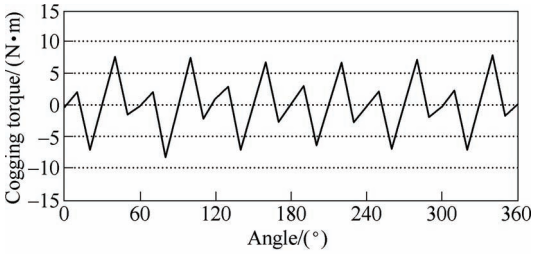

(a) RF-FSDC

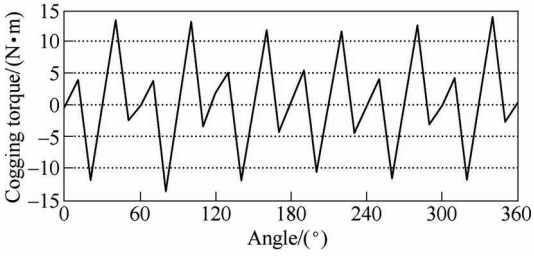

(b) AF-FSDC

Fig.14 Cogging torques at boosted conditions

Table 2 Key machine comparison

	RF-FSPM	RF-FSDC	AF-FSDC
Rated torque/(N·m)	202.3	98.1	152.4
Rated torque ripple(%)	12.8	17.6	15.1
Rated cogging torque/(N·m)	10.1	4.8	7.7
rated cogging torque(%)	5.0	4.9	5.1
Boosted torque/(N·m)	N/A	114.2	181.6
Boosted torque ripple	N/A	23.2 %	21.2 %
Boosted cogging torque/(N·m)	N/A	8.1	14.1
Boosted cogging torque(%)	N/A	7.1	7.7
Material cost/ USD	350.8	104.4	135.5
Rated torque / cost/(N·m/US)	0.6	0.9	1.1
Boosted torque /cost/(N·m/US)	N/A	1.1	1.3
Flux controllability	Low	High	High
Operating range	Narrow	Wide	Wide

all these machines are listed in Table 2. With the installation of the PM materials, the RF-FSPM machine can provide the highest rated torque performances, while regarding to the cost-effectiveness, its advantage is offset by the high material cost. On the other hand, without the employment of the PM materials, the magnetless AF-FSDC machine can enjoy the highest cost-effectiveness advantage among its counterparts.

5 Conclusion

In this paper, three representative FS machines, namely the RF-FSPM machine, the RF-FSDC machine and the AF-FSDC machine have been thoroughly analyzed and quantitatively compared. With the employment of the high-energy-density PM materials, the RF-FSPM machine can definitely offer the best power and torque density as compared with its magneltess counterparts. On the utilization of the radial area as active part for torque production, the AF-FSDC machine can produce comparable torque performance, while better cost-effectiveness than its PM counterpart does. In the meantime, the advanced magnetless FSDC machines can utilize their independent DC-field excitation for flux regulation, so that higher control flexibility can be accomplished for various situations.

References

[1] C. C. Chan, "The state of the art of electric, hybrid and fuel cell vehicles," *Proc. IEEE*, vol. 95, no. 4, pp. 704-718, Apr. 2007.

[2] K. T. Chau, W. Li, and C. H. T. Lee, "Challenges and opportunities of electric machines for renewable energy," *Progress In Electromagnetics Research B (Invited Paper)*, vol. 42, pp. 45-74, 2012.

[3] K. T. Chau, *Electric Vehicle Machines and Drives- Design, Analysis and Application*. New Jersey, USA: Wiley-IEEE Press, 2015.

[4] Z. Q. Zhu, and D. Howe, "Electrical machines and drives for electric, hybrid, and fuel cell vehicles," *Proc. IEEE*, vol. 95, no. 4, pp. 746-765, Apr. 2007.

[5] K. T. Chau, C. C. Chan, and C. Liu, "Overview of permanent-magnet brushless drives for electric and hybrid electric vehicles," *IEEE Trans. Ind. Electron*., vol. 55, no. 6, pp. 2246-2257, Jun. 2008.

[6] M. Cheng, W. Hua, J. Zhang, and W. Zhao, "Overview of stator-permanent magnet brushless machines," *IEEE Trans. Ind. Electron*., vol. 58, no. 11, pp. 5087-5101, Nov. 2011.

[7] E. Hoang, A. H. Ben-Ahmed, and J. Lucidarme, "Switching flux permanent magnet polyphased machines," in *Proc. Eur. Conf. Power Electron*. Appl., 1997, pp. 903-908.

[8] J. T. Chen, and Z. Q. Zhu, "Winding configurations and optimal stator and rotor pole combination of flux- switching PM brushless AC machines," *IEEE Trans. Energy Convers.*, vol. 25, no. 2, pp. 293-302, Jun. 2010.

[9] R. P Deodhar, A. Pride, S. Iwasaki, and J. J. Bremner, "Performance improvement in flux-switching PM machines using flux diverters," *IEEE Trans. Ind. Appl*., vol. 50, no. 2, pp. 937-978, Mar./Apr. 2014.

[10] C. H. T. Lee, K. T. Chau, C. Liu, D. Wu, and S. Gao, "Quantitative comparison and analysis of magnetless machines with reluctance topologies," *IEEE Trans. Magn.*, vol. 49, no. 7, pp. 3969-3972, Jul. 2013.

[11] I. Boldea, L. N. Tutelea, L. Parsa, and D. Dorrell, "Automotive electric propulsion systems with reduced or no permanent magnets: An overview," *IEEE Trans. Ind. Electron*., vol. 61, no. 10, pp. 5696-5711, Oct. 2014.

[12] C. H. T. Lee, K. T. Chau, and C. Liu, "Design and Analysis of a cost-effective magnetless multi-phase flux-reversal DC-field machine for wind power genera- tion," *IEEE Trans. Energy Convers.*, vol. 30, no. 4, pp. 1565-1573, Dec. 2015.

[13] D. Dorrell, L. Parsa, and I. Boldea, "Automotive electric motors, generators, and actuator drive systems with reduced or no permanent magnets and innovative design concepts," *IEEE Trans. Ind. Electron*., vol. 61, no. 10, pp. 5693-5695, Oct. 2014.

[14] C. H. T. Lee, K. T. Chau, and C. Liu, "Design and analysis of a dual-mode flux-switching doubly salient DC-field magnetless machine for wind power harves- ting," *IET Renew. Power Gener.*, vol. 9, no. 8, pp. 908-915, Apr. 2015.

[15] C. Yu, and S. Niu, "Development of a magnetless flux switching machine for rooftop wind power generation," *IEEE Trans. Energy Convers*., vol.30, no.4, pp. 1703- 1711, Dec. 2015.

[16] F. Profumo, Z. Zhang, and A. Tenconi, "Axial flux machines drives: A new viable solution for electric cars," *IEEE Trans. Ind. Electron*., vol. 44, no. 1, pp. 39-45, Feb. 1997.

[17] S. C. Oh, and A. Emadi, "Test and simulation of axial flux-motor characteristics for hybrid electric vehicles," *IEEE Trans. Veh. Technol*., vol. 53, no. 3, pp. 912-919, May 2004.

[18] C. H. T. Lee, K. T. Chau, C. Liu, T. W. Ching and F. Li, "A high-torque magnetless axial-flux doubly- salient machine for in-wheel direct drive applications," *IEEE Transactions on Magnetics*, vol. 50, no. 11, p. 8202405, Nov. 2014.

[19] Z. Nasiri-Gheidari, and H. Lesani, "Investigation of characteristics of a single-phase axial flux induction motor using three-dimensional finite element method and d-q model," *IET Electr. Power Appl.,* vol. 7, no. 1, pp. 47-57, Sept. 2012.

[20] R. Madhavan, and B. G. Fernandes, "Axial flux segmented SRM with a higher number of rotor segments for electric vehicles," *IEEE Trans. Energy Convers*., vol. 28, no. 1, pp. 203-213, Mar. 2013.

[21] C. H. T. Lee, C. Liu, and K. T. Chau, "A magnetless axial-flux machine for range-extended electric vehicle," *Energies*, vol. 7, no. 3, pp. 1483-1499, Mar. 2014.

Christopher H. T. Lee received the B.Eng. (First Class Hons.) degree in electrical engineering from Department of Electrical and Electronic Engineering, University of Hong Kong, Hong Kong, in 2009. He has been working toward the Ph.D. degree since 2011. During the Ph.D. study, he was co-supervised by Prof. K. T. Chau and Prof. C. C. Chan. His research interests include electric machines and drives, renewable energies, and electric vehicle technologies. In these areas, he has published about 30 technical papers. (http://www.eee.hku.hk/~htlee/)

K. T. Chau received the B.Sc.(Eng.) with 1st Class Hons, M.Phil., and Ph.D. degrees in electrical and electronic engineering from The University of Hong Kong, Hong Kong, in 1988, 1991, and 1993, respectively. Since 1995, he has been with The University of Hong Kong, where he is currently a Professor in the Department of Electrical and Electronic Engineering. He has published 6 books, 8 book chapters and over 250 refereed journal papers. His research interests include electric and hybrid vehicles, machines and drives, and renewable energy systems. Professor Chau is Fellow of the IEEE, IET and HKIE. He currently serves as Co-editor of the Journal of Asian Electric Vehicles. He was the recipient of the Changjiang Chair Professorship from the Ministry of Education, China, the Environmental Excellence in Transportation Award for Education, Training, and Public Awareness from the SAE International, and the Award for Innovative Excellence in Teaching, Learning and Technology at the International Conference on College Teaching and Learning. (http://www.eee.hku.hk/people/ktchau/)

Prof. C. C. Chan holds BSc, MSc, PhD, HonDSc, HonDTech degrees. Honorary Professor and Former Head of the Department of Electrical and Electronic Engineering at the University of Hong Kong; Visiting Professor of MIT, University of Cambridge, etc; Founding President of the World Electric Vehicle Association; Senior Consultant to governments, Strategic Adviser or Independent Director of public companies and industries; Fellow of the Royal Academy of Engineering, U.K., Chinese Academy of Engineering, IEEE, IET and HKIE. Recipient of the Royal Academy of Engineering Prince Philip Medal; World Federation of Engineering (WFEO) Medal of Engineering Excellence; Gold Medal of Hong Kong Institution of Engineers; IEE International Lecture Medal; "Asia's Best Technology Pioneers" by Asiaweek; "Father of Asian Electric Vehicles" by Magazine Global View; "Pitamaha (Grandfather) of Electric Vehicle Technology" in India; "Environmental Excellence in Transportation Award" by Society of Automotive Engineers (SAE); published 11 books, over 300 technical papers and holds 9 patents. (http://www.eee.hku.hk/people/ccchan.html)